Available online at www.sciencedirect.com

ScienceDirect

Ceramics International 39 (2013) 9397–9403

CERAMICS INTERNATIONAL

www.elsevier.com/locate/ceramint

Effect of holmium substitution on electrical properties of strontium bismuth tantalate ferroelectric ceramics

Sugandha[a], A.K. Jha[a,b,*]

[a]Thin Film and Material Science Laboratory, Department of Applied Physics, Delhi Technological University (Formerly Delhi College of Engineering), Delhi 110042, India

[b]Department of Applied Sciences, A.I.A.C.T.R., Geeta Colony, Delhi 110031, India

Received 28 February 2013; received in revised form 5 May 2013; accepted 11 May 2013
Available online 27 May 2013

Abstract

The holmium substituted $SrBi_{2-x}Ho_xTa_2O_9$ ($x=0.00$–2.0) compositions were synthesized by the solid state reaction method. The synthesized specimens were characterized for their structural and electrical properties. X-ray diffractograms reveal single phase layered perovskite structure formation for holmium content up to $x\leq 0.1$. The variation of dielectric constant with temperature shows that the Curie temperature (T_c) decreases on increasing the holmium content. The specimen with $x=2.0$ i.e. the bismuth free specimen, has very low dielectric constant and does not show any appreciable variation with temperature. The dielectric loss reduces significantly with holmium substitution. The ferroelectric property has been observed to improve with Ho substitution. The specimen with $x=0.01$ exhibits highest remnant polarization ($P_r=9.22$ μC/cm^2) while the bismuth free specimen shows the lowest value of remnant polarization. It is expected that the above ferroelectric materials can be used to replace static (SRAM) and dynamic (DRAM) random access memories with ferroelectric random access memories (FeRAMS).

Keywords: A. Solid state reaction; B. Electron microscopy; C. Ferroelectric properties; D. Perovskites

1. Introduction

A large number of ferroelectric materials have been intensely investigated for applications in non-volatile ferroelectric random access memories (FeRAMs), piezoelectric transducers, actuators, pyroelectric sensors, high dielectric constant capacitors, etc. [1–5]. Among various ferroelectric materials, lead zirconate titanate (PZT) has been regarded as the best potential material for memory device applications because of its superior ferroelectric properties [6,7]. However, PZT has limitations such as environmentally hazardous lead content, high leakage current and poor fatigue endurance [8]. The bismuth layered ferroelectric materials such as strontium bismuth tantalate (SBT) has attracted a lot of attention of the researchers as an alternative ferroelectric material to PZT. In addition to being lead free, it has various other advantages such as low leakage current and high fatigue endurance up to 10^{12} switching cycles [9–12]. Therefore, it is important to find alternative lead free ferroelectric material exhibiting superior ferroelectricity comparable to PZT.

SBT is a member of bismuth layer structured ferroelectric material with a general formula of $(Bi_2O_2)^{2+}$ $(A_{n-1}B_nO_{3n+1})^{2-}$, where A=$Ca^{2+}$, Ba^{2+}, Sr^{2+}, Bi^{3+}, La^{3+}, Sm^{3+}, etc. and B=Fe^{3+}, Ti^{4+}, Nb^{5+}, Ta^{5+}, W^{6+}, Mo^{6+}, etc; and n indicates the number of corner sharing octahedra forming the perovskite like slabs [13,14]. The crystal structure of $SrBi_2Ta_2O_9$ comprises of pseudo-perovskite blocks $(SrTa_2O_7)^{2-}$ that are sandwiched between $(Bi_2O_2)^{2+}$ layers. Sr atom occupies the A-site of the perovskite blocks and Ta atoms occupy the B-site. However, pure SBT suffers from various major limitations such as high dielectric loss, low remnant polarization values, high processing temperature, bismuth volatilization, etc. [15–17]. Significant efforts have been made to improve the dielectric and ferroelectric properties of this compound. It has been reported that substitution by various cations at A-site or B-site or Bi_2O_2 layer can effectively enhance the physical and chemical properties of parent SBT structure for various device applications [18–22].

*Corresponding author at: Department of Applied Sciences, A.I.A.C.T.R, Geeta Colony, Delhi 110031, India. Tel.: +91 98 68 24 21 50; fax: +91 11 27 87 10 23.
E-mail address: prof.akjha@gmail.com (A.K. Jha).

0272-8842/$ - see front matter © 2013 Elsevier Ltd and Techna Group S.r.l. All rights reserved.
http://dx.doi.org/10.1016/j.ceramint.2013.05.056

Several investigations have indicated that the defects such as oxygen vacancies accumulate near the grain boundaries leading to strong domain pinning. This results in decrease in remnant polarization [23,24]. Therefore it is essential to control the defects in perovskite blocks and Bi_2O_2 layer to obtain improved ferroelectric properties. Many investigations on $Bi_4Ti_3O_{12}$ (BIT) indicated that the substitution of rare earth ions for volatile bismuth ion was effective in suppressing the concentration of oxygen vacancies. For instance, it has been reported that La doped BIT exhibited enhanced Pr value [25]. In addition, Chon et al. reported that the Sm doped BIT thin films show excellent fatigue free characteristics and very large $2P_r$ value of 49 C/μcm^2 [26]. Similarly, Srinivas et al. reported that substitution of Sm, Gd and Dy rare earth ions in Bi_2O_2 layer of SBT lattice resulted in enhanced dielectric and ferroelectric properties [27].

Detailed literature survey revealed that even though a lot of work has been done on pristine SBT compound, hardly any systematic work dealing with the characterization of rare earth Ho substituted SBT as a function of composition has been reported. This prompted the authors to synthesize the holmium containing $SrBi_{2-x}Ho_xTa_2O_9$ ($x=0.0$–2.0) compounds and investigate their structural and electrical properties.

2. Experimental technique

$SrBi_{2-x}Ho_xTa_2O_9$ compositions with $x=0.0$, 0.01, 0.025, 0.05, 0.075, 0.1, 0.5 and 2.0 were synthesized by the solid-state reaction method taking $SrCO_3$, Bi_2O_3, Ta_2O_5 and Ho_2O_3 (all from Aldrich purity 99.9%) in their stoichiometric proportions. The powder mixtures were thoroughly grounded and passed through a sieve of appropriate size and then calcined at 900 °C in air for 2 h. The calcined mixtures were grounded and admixed with 1.5 wt% polyvinyl alcohol (Aldrich) as a binder and then pressed at 300 MPa into disk shaped pellets. The pellets were sintered at 1200 °C for 2 h in air.

X-ray diffractograms of the sintered pellets were recorded using a Bruker diffractometer (model D8 Advance) in the range $20°\leq 2\theta \leq 70°$ with Cu Kα radiation($\lambda=1.5405$ Å) at a scanning rate of 1°/min. The granular morphology was investigated using scanning electron microscope (Hitachi, S-3700N). The sintered pellets were polished and silver paste was applied on both sides and cured at 500 °C for 1 h. The dielectric measurements were carried out using a precision LCR meter (Agilent 4284A) operating at oscillation amplitude of 1 V. The polarization–electric field (P–E) hysteresis loops

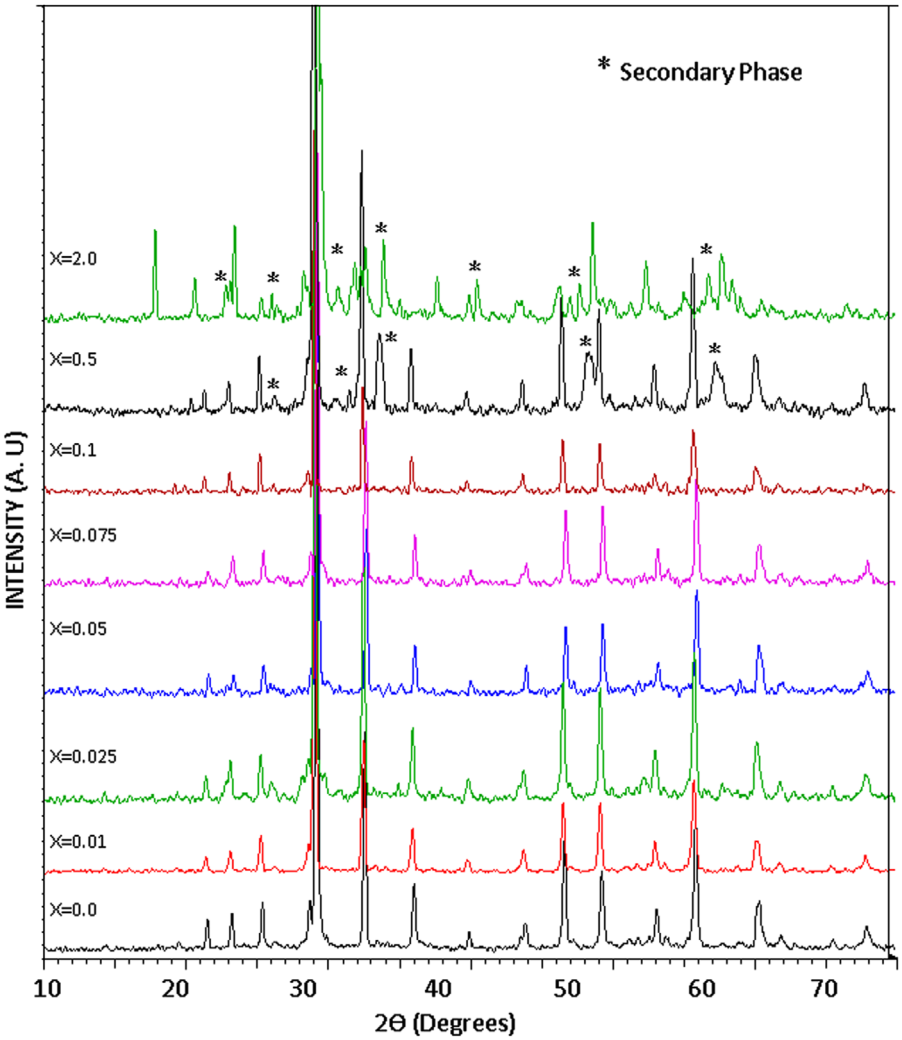

Fig. 1. X-ray diffraction patterns of $SrBi_{2-x}Ho_xTa_2O_9$($x=0.0$–2.0) compounds.

were recorded using a *P–E* loop tracer based on Sawyer–Tower circuit.

3. Results and discussions

Fig. 1 shows the XRD patterns of the sintered samples. The XRD peaks are similar to those in the standard diffraction pattern of $SrBi_2Ta_2O_9$ on the JCPDS card (JCPDS file no.-072-7073) for the samples up to $x \leq 0.1$. Further, the specimens remain single phase up to $x \leq 0.1$ suggesting the incorporation of Ho atoms at Bi site in the SBT lattice. However, for $x > 0.1$, additional peaks are also observed indicating the formation of secondary phase. A comparison of the additional peaks with standard XRD patterns of JCPDS file no.-024-0478 shows the formation of $HoTaO_4$ as the secondary phase. Lattice parameters were calculated from the XRD patterns using a powder-X software package [28] and are listed in Table 1. A decrease in lattice parameters with increasing Ho substitution is observed which can be understood as the ionic radius of Ho^{3+} (0.91 Å) is smaller than that of Bi^{3+} (0.96 Å) [29].

It is known that the composition and sintering temperature influences the microstructure such as grain growth and densification of the specimen, which in turn control other properties of the material [30–32]. The effect of Ho substitution on the microstructure has been examined using SEM and the obtained micrographs are shown in Fig. 2. It is clearly observed that Ho substitution has pronounced effect on the average grain size, density and homogeneity of the grains. Table 1 lists the average grain size for all the synthesized specimens. The sample with $x=0.01$ has higher grain size compared to Ho free SBT. However, beyond $x > 0.01$ the average grain size decreases gradually with increasing Ho content. Further, sample with $x=0.01$ exhibits homogeneous microstructure with well defined grains and grain boundaries compared to other specimens with higher holmium content. The above observed behavior can be explained as follows. It is well known that the diffusion coefficient is directly proportional to the sintering temperature and inversely proportional to the radius of the diffusing ion [33,34]. Therefore, in the present study, it is expected that for $x > 0.01$ lower sintering temperature might have been required for the diffusion of small sized Ho^{3+} ions (I.R. −0.91 Å) into Bi^{3+} (I.R. −0.96 Å) site. However, in all the specimens the sintering temperature was the same (1200 °C). Therefore, it is possible that at this sintering temperature in the higher holmium containing specimens, Ho^{3+} atoms segregate at the grain boundaries progressively inhibiting grain growth [35,36].

3.1. Dielectric studies

Fig. 3 illustrates the variation of the dielectric constant (Fig. 3(a)) and dielectric loss (Fig. 3(b)) with temperature at a frequency of 100 kHz. The following observations can be made from Fig. 3(a). Firstly, the compound with $x=0.0$–0.5 undergo ferroelectric–paraelectric phase transition of diffuse type at the Curie temperature (T_c), whereas the specimen with $x=2.0$ i.e. the bismuth free composition does not show any dielectric anomaly in the studied temperature range. Secondly, the Curie temperature (T_c) is observed to decrease with increase in holmium concentration upto $x=0.5$. However, specimen with $x=2.0$ does not exhibit transition temperature values. Thirdly, the specimen with $x=0.01$ exhibits higher value of dielectric constant ($\varepsilon_{max}=279.53$) as compared to Ho free SBT ($\varepsilon_{max}=212.74$) and thereafter dielectric constant decreases continuously. The observed behavior can be explained as follows.

The broad dielectric peak in Fig. 3(a), indicates that the transition in the compositions within $0.0 \leq x \leq 0.5$ is of the diffuse type, an important characteristic of a disordered perovskite structure [37]. The diffuseness of the peak can be calculated by diffusivity constant (γ) using the empirical relation [38].

$$\ln(1/\varepsilon - 1/\varepsilon_{max}) = \gamma \ln(T - T_c) + \text{constant}$$

where ε_{max} is the maximum value ε at $T=T_c$. The values of γ at 100 kHz for all the samples are obtained from the slope of $\ln[(1/\varepsilon)-(1/\varepsilon_{max})]$ versus $\ln[T-T_c]$ curve and are listed in Table 1. For all the studied composition, γ is found to be between 1 (obeying Curie–Weiss law) and 2 (for completely disordered system) confirming the diffuse phase transition nature in the specimen. The value of γ is observed to decrease from Ho free ($x=0.0$) to $x=0.01$ composition, however, it increases as the concentration of holmium is further increased. This suggests that sample with $x=0.01$ is more ordered than other compositions and disorderness increases as holmium content is increased in the specimens.

The observed higher dielectric constant for $x=0.01$ can be understood on the basis of the variation of grain size of the synthesized specimens [39]. It is well known that in most cases

Table 1
Variation of different parameters of $SrBi_{2-x}Ho_xTa_2O_9$ ($x=0.0$–2.0) compounds.

x	a (Å)	b (Å)	c (Å)	ε_{max} (100 KHz)	Grain size (μm)	P_r (μC/cm^2)	Diffusivity (γ)	T_c (°C)
0.0	5.4983	5.5131	24.9688	212.374	2.33	2.55	1.326	335
0.01	5.4963	5.5126	24.8352	279.530	5.62	9.22	1.304	250
0.025	5.4928	5.5121	24.7894	157.717	4.13	6.39	1.367	185
0.05	5.4878	5.5111	24.6201	126.246	3.53	4.99	1.518	175
0.075	5.4848	5.4984	24.2928	104.735	3.13	2.47	1.794	155
0.1	5.4812	5.4968	24.0114	94.501	2.47	2.02	1.797	150
0.5	5.4809	5.4962	23.9728	82.761	2.15	1.86	1.797	142
2.0	5.4809	5.4959	23.9691	–	1.67	0.36	–	–

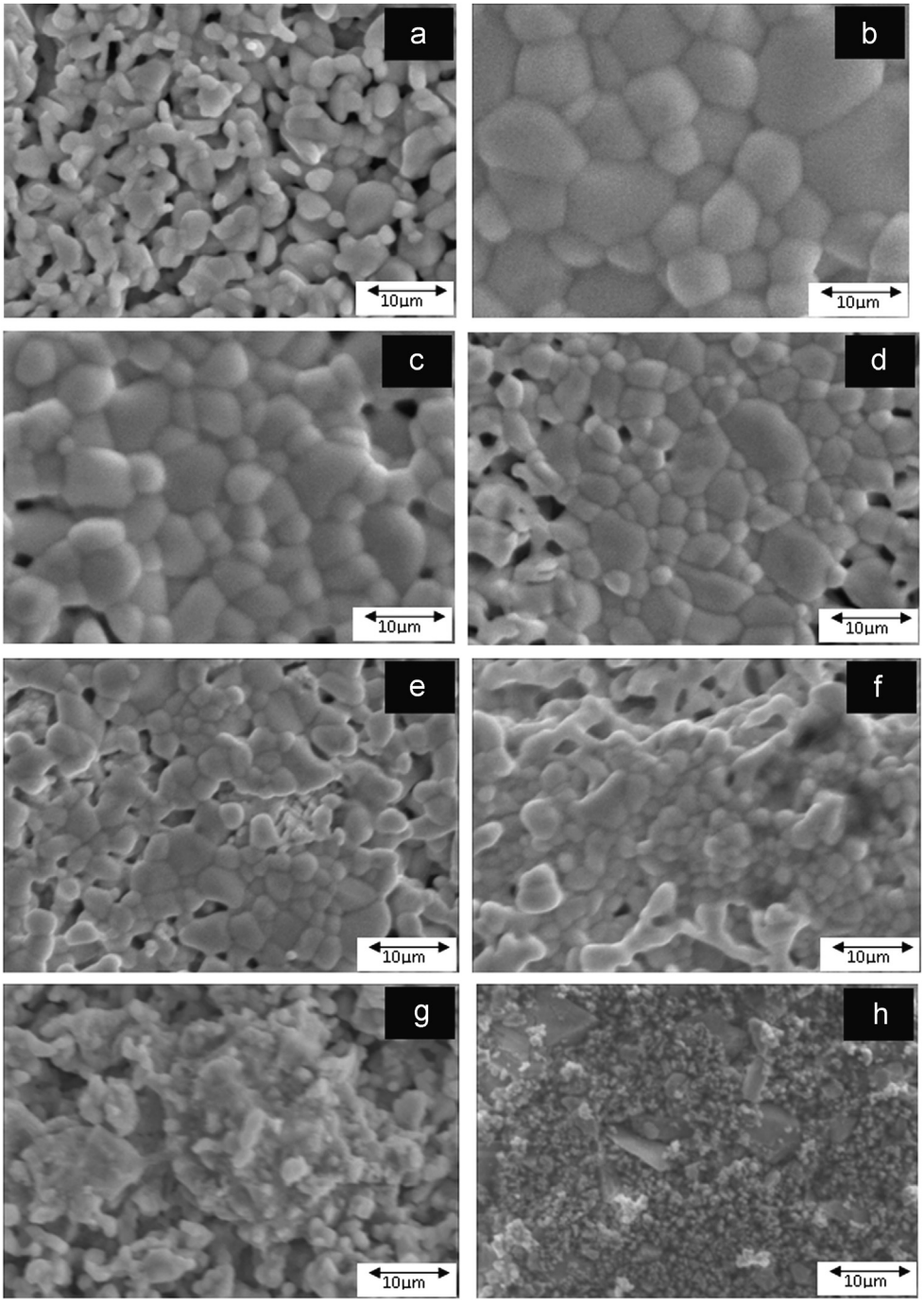

Fig. 2. SEM micrographs of $SrBi_{2-x}Ho_xTa_2O_9$ [(a) $x=0.0$, (b) $x=0.01$, (c) $x=0.025$, (d) $x=0.05$, (e) $x=0.075$, (f) $x=0.1$, (g) $x=0.5$, and (h) $x=2.0$].

the dielectric constant of the ferroelectric materials depends upon the composition, grain size, secondary phases etc. [40–42]. As observed in the SEM micrographs (Fig. 2(a and b)), the specimen with $x=0.01$ exhibits enhanced microstructure with higher grain size as compared to the holmium free SBT specimen. Higher grain size facilitates easier domain wall motion resulting into higher dielectric constant values [43–45]. However, beyond $x>0.01$, dielectric constant decreases with increase in holmium content. This is possibly due to comparatively smaller grains as observed in Table 1 [46–49]. Also, the decrease in dielectric constant values can also be attributed to the porous microstructure and presence of secondary phases, which is indeed observed in Figs. 1 and 2 (c–h) [50,51]. Further, it is observed that sample with x=0.025 and 0.05 exhibit higher grain size and lower dielectric constant values as compared to holmium free sample. It is known that higher grain size facilitates higher dielectric constant values; however grain size and porosity are not the only factors which determine the net dielectric constant of the specimen. Therefore the observed variation is possibly due to the decrease in the net polarization in the holmium containing compounds as the ionic polarizabilty of Ho^{3+} (3.97 $Å^3$) is lower than that of

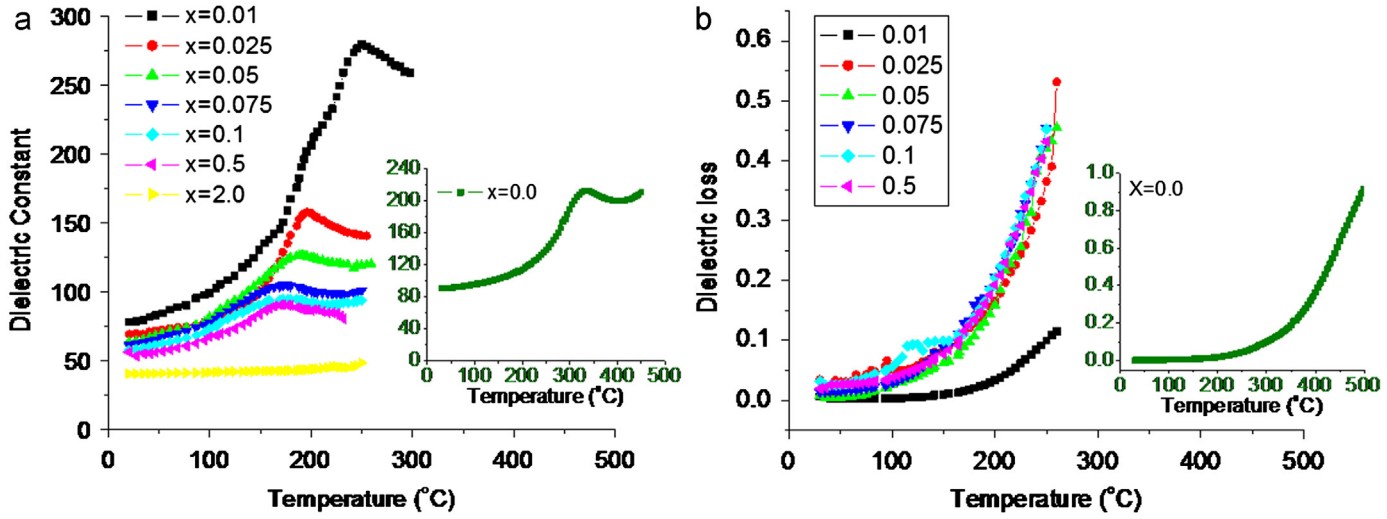

Fig. 3. (a) Variation of dielectric constant and (b) dielectric loss with temperature of $SrBi_{2-x}Ho_xTa_2O_9$(x=0.0–2.0) compounds.

Bi^{3+}(6.12 Å^3) [52,53]. This results in lowering of dielectric permittivity in the specimen as indeed observed. It is also important to note that in the specimen with x=2.0, there is almost no variation in the dielectric constant with temperature signifying the importance of Bi_2O_2 layer in these perovskite structures. It is expected that the above behavior will have implications on ferroelectric property as discussed later.

The decrease in Curie temperature (T_c) in Ho substituted samples can be explained on the basis of decrease in structural distortion [54,47]. This is due to the fact that in SBT structure there exist strong hybridization between Bi 6s and O 2p orbit. In Bi_2O_2 layer, Bi^{3+} ions with lone pair 6s electron bonds covalently with O^{2-} ions resulting into drastic distortion of the pseudo-perovskite blocks [55,56]. When holmium ion without 6s electron occupies the Bi site, the structural distortion relives resulting into decrease in T_c [47]. The observed dielectric behavior is the cumulative effect of all the above discussed causes.

Fig. 3(b) shows the dielectric loss (at 100 kHz) as a function of temperature for the studied specimens. It is observed that dielectric loss reduces significantly on holmium substitution. Further, sample with x=0.01 exhibit minimum loss values as compared to other compositions. The source of dielectric loss in these ceramics is space charge polarization/domain wall relaxation [57]. The presence of defects like oxygen vacancies, V••, act as space charge and contribute to the dielectric loss in these materials [58]. It is known that the pristine $SrBi_2Ta_2O_9$ is not perfectly stoichiometric, but contains a certain amount of inherent defects (e.g. oxygen vacancies) resulting from the volatilization of Bi_2O_3 at high temperatures [59]. When Bi_2O_3 is lost, bismuth and oxygen vacancy complexes are formed in the $(Bi_2O_2)^{2+}$ layers. It has been established through X-ray photoemission spectroscopy studies that the oxygen ions in $(Bi_2O_2)^{2+}$ layers are less stable than the O^{2-} ions in $(SrTa_2O_7)^{2-}$ perovskite slabs [59,60]. Many investigations of $Pb(Zr,Ti)O_3$ have indicated that the defects such as oxygen vacancies, V••, act as space charge which plays an important role in increase of dielectric loss in the perovskite materials [61]. Therefore, substitution of Ho atoms into Bi_2O_2 layer reduces the number of oxygen vacancies resulting into lower loss values.

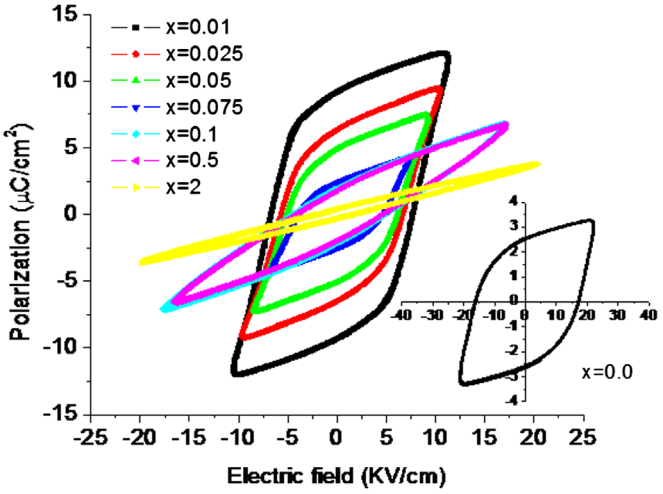

Fig. 4. P–E hysteresis loops of $SrBi_{2-x}Ho_xTa_2O_9$(x=0.0–2.0) compounds at room temperature.

3.2. Ferroelectric properties

To confirm the ferroelectric nature of the studied compounds, hysteresis loops were recorded at room temperature at a frequency of 100 Hz. Fig. 4 shows the variation of polarization as a function of applied electric field for all the studied samples. Table 1 lists the values of remnant polarization (P_r) for all the samples. It is observed that the P_r value increases with holmium substitution. Further, the sample with x=0.01 exhibit well saturated P–E loop with highest remnant polarization value (9.22 μC/cm^2) and thereafter P_r values decreases at higher holmium concentrations. The observed behavior can be explained as follows.

It is well known that the polarization switching behavior of ferroelectric materials is strongly influenced by defects like

oxygen vacancies [62]. These oxygen vacancies assemble near domain walls and thus the polarization reversal of these domains is suppressed due to "pinning" by these defects near the domain boundaries resulting in smaller remnant polarization values [63]. There is sufficient experimental evidence to indicate that the defects accumulated at electrode-ferroelectric interfaces (or grain and domain boundaries) are mainly oxygen vacancies which have a direct effect on the ferroelectric properties [64–66]. In the present case, the observed ferroelectric behavior can be understood in terms of the reduction in the number of oxygen vacancies. As discussed earlier, the pure SBT sample has inherent oxygen vacancies resulting from the volatilization of Bi_2O_3, whereas partial substitution of holmium atoms into Bi_2O_2 layer effectively reduces the number of oxygen vacancies. This is consistent with the observation of enhanced ferroelectric properties in holmium substituted samples. Further, the decrease in remnant polarization values for samples beyond $x > 0.01$ can be attributed to the decrease in grain size and comparatively porous microstructure [67,68]. Also, it is important to note that the specimen with $x=2.0$, exhibit negligible remnant polarization value ($P_r=0.36$ μC/cm^2). This reveals the importance of Bi_2O_2 layer in these perovskite compounds. While there is a significant reduction in the P_r value nevertheless this bismuth free specimen have a finite low value of P_r.

4. Conclusion

A single phase layered perovskite structure is maintained in $SrBi_{2-x}Ho_xTa_2O_9$ (SBHT) samples up to $x=0.1$ and secondary phases appear for higher holmium content. Higher dielectric constant value is observed for the specimen with $x=0.01$ and thereafter dielectric constant decreases. The Curie temperature decreases with increase in holmium content and the dielectric loss reduces significantly. The ferroelectric property enhances on Ho substitution. The maximum P_r value of ~9.22 μC/cm^2 is obtained for $x=0.01$. Also, degraded dielectric and ferroelectric behavior is observed in the bismuth free specimen with $x=2.0$.

References

[1] S.B. Desu, D.P. Vijay, Novel fatigue-free layered structure ferroelectric thin films, Materials Science and Engineering B 32 (1995) 75.

[2] J.F. Scott, F.M. Ross, C.A. Araujo, M.C. Scott, M. Huffman, Ferroelectric thin films: review of materials, properties, and applications, Materials Research Society Bulletin 21 (1996) 1–5.

[3] K. Takemura, T. Noguchi, M. Miyasaka, Dielectric anomaly in strontium bismuth tantalate thin films, Applied Physics Letters 73 (12) (1998) 1649–1651.

[4] R.R. Neurgaonkar, W.F. Hall, J.R. Oliver, W.W. Ho, W.K. Cory, Ferroelectric properties of tetragonal tungsten bronze single crystals, Ferroelectrics 56 (1984) 31–36.

[5] Sugandha, A.K. Jha, Nanocrystalline non-stoichiometric SBT: effect of milling duration on structural and electrical characteristics, Materials Characterization 65 (2012) 126–132.

[6] B.H. Park, B.S. Kang, S.D. Bu, T.W. Noh, W. Jo, Lanthanum-substituted bismuth titanate for use in non-volatile memories, Nature 401 (1992) 682.

[7] D. Wu, A. Li, T. Zhu, Z. Liu, N. Ming, Ferroelectric properties of $Bi_{3.25}La_{0.75}Ti_3O_{12}$ thin films prepared by chemical solution deposition, Journal of Applied Physics 88 (2000) 5941.

[8] H. Watanabe, T. Mihara, H. Yoshimori, C.A.P. De Araujo, Preparation of ferroelectric thin films of bismuth layer structured compounds, Japanese Journal of Applied Physics 34 (1995) 5240.

[9] C.A.P. de Araujo, J.D. Cuchlaro, L.D. Mcmillan, M.C. Scott, J.F. Scott, Fatigue-free ferroelectric capacitors with platinum electrodes, Nature 374 (1995) 627.

[10] R. Jain, V. Gupta, K. Sreenivas, Sintering characteristics and properties of sol gel derived $Sr_{0.8}Bi_{2.4}Ta_{2.0}O_9$ ceramics, Materials Science and Engineering B 78 (2000) 63.

[11] L.S. Zheludev, Physics of Crystalline Dielectrics, Electrical Properties, vol. 2, Plennum, New york474.

[12] V. Shrivatava, A.K. Jha, R.G. Mehdiratta, Structural distortion and phase transition studies of Aurivillius type $Sr_{1-x}Pb_xBi_2Nb_2O_9$ ferroelectric ceramics, Solid State Communications 133 (2004) 125.

[13] B. Aurivillius, Dielectric relaxation in layered oxides of the Aurivillius phase family, Arkiv foer Kemi 1 (1949) 463.

[14] E.C. Subbaro, A family of ferroelectric bismuth compounds, Journal of Physics and Chemistry of Solids 23 (1962) 665.

[15] J.F. Scott, High dielectric constant thin films for dynamic random access memories (DRAM), Annual Review of Materials Science 28 (1998) 79.

[16] F. Kulcsar, Electromechanical properties of lead titanate zirconate ceramics modified with certain three-or five-valent additions, Journal of American Ceramic Society 42 (1959) 343.

[17] A. Li, D. Wu, H. Ling, T. Yu, X. Yin, N. Ming, Effect of excess bismuth on the microstructures and electrical properties of strontium bismuth tantalate (SBT) thin films, Thin Solid Films 375 (2000) 215.

[18] R.B. Atkin, R.L. Holman, R.M. Fulrath, Substitution of Bi and Nb ions in lead zirconate–titanate, Journal of the American Ceramic Society 54 (1971) 113.

[19] P. Duran Martin, A. Catro, P. Millan, R. Jimnez, Influence of Bi-site substitution on the ferroelectricity of the Aurivillius compound $Bi_2SrNb_2O_9$, Journal of Materials Research 13 (1998) 2565.

[20] R.R. Das, P. Bhattacharya, W. Perez, R.S. Katiyar, S.B. Desu, Ferroelectric properties of laser-ablated $Sr_{1-x}A_xBi_2Ta_2O_9$ thin films (where A = Ba, Ca), Applied Physics Letters 80 (2002) 637.

[21] T.J. Boyle, P.G. Clem, B.A. Juttle, T.D. Dunbarb, W.F. Hammetter, Structural and electrical properties of $SrBi_2V_xNb_{2-x}O_9$ ferroelectric ceramics: effect of temperature and frequency, Journal of Materials Research 17 (2002) 4.

[22] S. Sahoo, R.N.P. Choudhary, B.K. Mathur, Structural, ferroelectric and impedance spectroscopy properties of Y^{3+} modified $Pb(Fe_{0.5}Nb_{0.5})O_3$ ceramics, Physica B 406 (2011) 1660–1664.

[23] Y. Noguchi, I. Miwa, M. Miyayama, Japanese Journal of Applied Physics 39 (2000) L125.

[24] H. Watanabe, T. Mihara, C.A.P. Araujo, Japanese Journal of Applied Physics 34 (1995) 5240.

[25] J.C. Bae, S.S. Kim, E.K. Choi, T.K. Song, Y. Lee, Ferroelectric properties of lanthanum-doped bismuth titanate thin films grown by a sol–gel method, Thin Solid Films 472 (2005) 90–95.

[26] U. Chon, K.B. Kim, H.M. Jang, G.C. Yi, Applied Physics Letters 79 (2001) 3137.

[27] A. Srinivas, F.Y.C. Boey, T.J. Sritharan, Synthesis of a new electroceramic by replacement of Bi in strontium bismuth niobate, Journal of Electroceramics 16 (2006) 321.

[28] C. Dong, Windows-95-based program for powder X-ray diffraction data processing, Journal of Applied Crystallography 32 (1999) 838.

[29] R.D. Shannon, C.T. Prewitt, Effective ionic radii in oxides and fluorides, Acta Crystallographica B 25 (1965) 925.

[30] T. Atsuki, N. Soyama, T. Yonezawa, K. Ogi, Preparation of bi-based ferroelectric thin films by sol–gel method, Japanese Journal of Applied Physics 34 (1995) 5096.

[31] M. Noda, Y. Matsumuro, H. Sugiyama, M. Okuyama, A fatigue-tolerant metal–ferroelectric-oxide–semiconductor structure with large memory window using Sr-deficient and Bi-excess $Sr_{0.7}Bi_{2+y}Ta_2O_9$ ferroelectric films prepared on SiO_2/Si at low temperature by pulsed laser deposition, Japanese Journal of Applied Physics 38 (1999) 2275.

[32] Sugandha, A.K. Jha, Synthesis and characterization of nanocrystalline ferroelectric $Sr_{0.8}Bi_{2.2}Ta_2O_9$ by conventional and microwave sintering: a comparative study, Materials Research Bulletin 48 (2013) 1553–1559.
[33] K. Huang, Statistical Mechanics, Wiley, New York, 1987.
[34] P.A. Jha, A.K. Jha, Effect of sintering temperature on the grain growth and electrical properties of barium zirconate titanate ferroelectric ceramics, Journal of Materials Science: Materials in Electronics 24 (2013) 1511.
[35] K. Raman, K. Chandramouli, Effect of rare earth donor Ce^{3+} doping at A-site of PLSZNT on dielectric and piezoelectric properties, Current Applied Physics 9 (2009) 907–912.
[36] J.C. Bae, S.S. Kim, E.K. Choi, T.K. Song, Y. Lee, Ferroelectric properties of lanthanum-doped bismuth titanate thin films grown by a sol–gel method, Thin Solid Films 472 (2005) 90–95.
[37] R. Rai, S. Sharma, R.N.P. Choudhary, Structural and dielectric properties of Bi modified PLZT ceramics, Solid State Communications 133 (2005) 635.
[38] S.M. Pilgrim, A.E. Sutherland, S.R. Winzer, Diffuseness as a useful parameter for relaxor ceramics, Journal of the American Ceramic Society 73 (1990) 3122.
[39] C. Yichan, S. Yuming, L. Chiping, Enhanced a-axis-oriented crystal growth of Nd-substituted bismuth titanate thin films with layer-by-layer crystallization, Journal of Crystal Growth 268 (2004) 210.
[40] R.R. Das, P. Bhattacharya, W. Perez, R.S. Katiyar, Effect of electrolyte additives on sol-precipitated nano silica particles, Ceramics International 30 (7) (2004) 1175.
[41] E.C. Subbarao, Systematics of bismuth layer compounds, Integrated Ferroelectrics 12 (1996) 33.
[42] I. Coondoo, N. Panwar, A.K. Jha, Effect of sintering temperature on the structural, dielectric and ferroelectric properties of tungsten substituted SBT ceramics, Physica B 406 (2011) 374.
[43] H.T. Martirena, J.C. Burfoot, Grain-size effects on properties of some ferroelectric ceramics, Journal of Physics C: Solid State Physics 7 (1976) 3162.
[44] I. Coondoo, A.K. Jha, Investigations of structural, dielectric and ferroelectric behavior of europium substituted $SrBi_2Ta_2O_9$ ferroelectric ceramics, Solid State Communications 142 (2007) 561.
[45] A.K. Jha, Sugandha, Structural and dielectric investigations of bismuth excess strontium bismuth tantalate ferroelectric ceramics, Ferroelectrics 421 (2011) 1–8.
[46] Z.H. Bao, Y.Y. Yao, J.S. Zhu, Y.N. Wang, Study on ferroelectric and dielectric properties of niobium doped $Bi_4Ti_3O_{12}$ ceramics and thin films prepared by PLD method, Materials Letters 56 (2002) 861.
[47] F. Qiang, J.H. He, J. Zhu, X.B. Chen, Ferroelectric and dielectric properties of bismuth-layered structural $Sr_2Bi_{4-x}Ln_xTi_5O_{18}$ (Ln=La, Nd, Sm and Dy) ceramics, Journal of Solid State Chemistry 179 (2006) 1768.
[48] H. Huang, C.Q. Sun, Z.S. Tian, Grain-size effect on ferroelectric $Pb(Zr_{1-x}Ti_x)O_3$ solid solutions induced by surface bond contraction, Physical Review B 63 (2001) 184112.
[49] F. Suhua, C. Wen, H. Guangda, Effects of excess bismuth on structure and properties of $SrBi_4$ Ti_4O_{15} ceramics, Journal of Rare Earths 25 (2007) 317.
[50] P. Ganguly, A.K. Jha, Structural and electrical properties of $Ba_{5-x}Ca_xSmTi_3Nb_7O_{30}$ (x=0–5) ferroelectric ceramics, Journal of Alloys and Compounds 495 (2010) 7–12.
[51] K.K. Tae, K. Chang, Effect of bismuth excess on the crystallization of $Bi_{3.25}La_{0.75}Ti_3O_{12}$ thin films on $Pt/Ti/SiO_2/Si$ substrates, Microelectronic Engineering 71 (2004) 266.
[52] R.D. Shannon, Dielectric polarizabilties of ions in oxides and florides, Journal of Applied Physics 73 (1993) 348–366.
[53] P. Ganguly, A.K. Jha, Investigations of structural, dielectric and electrical behavior of calcium substituted $Ba_5NdTi_3Nb_7O_{30}$ ferroelectric ceramics, Integrated Ferroelectrics 113 (2010) 149–156.
[54] Y. Shimakawa, Y. Kubo, Y. Nakagawa, S. Goto, Crystal structure and ferroelectric properties of $ABi_2Ta_2O_9$(A=Ca, Sr, and Ba), Physical Review B 61 (2000) 6559.
[55] Y. Noguchi, M. Miyayama, T. Kudo, Effect of Bi substitution at the Sr site on the ferroelectric properties of dense strontium bismuth tantalate ceramics, Journal of Applied Physics 88 (2000) 2146.
[56] Y. Noguchi, M. Miyayama, T. Kudo, Direct evidence of A-site-deficient strontium bismuth tantalate and its enhanced ferroelectric properties, Physical Review B 63 (2001) 214102.
[57] I.S. Zheludev, Physics of Crystalline Dielectrics, Electrical Properties, vol. 2, Plenum, New York474.
[58] Y. Noguchi, M. Miyayama, Large remanent polarization of vanadium doped $Bi_4Ti_3O_{12}$, Applied Physics Letters 78 (2001) 1903.
[59] B.H. Park, S.J. Hyun, S.D. Bu, T.W. Noh, J. Lee, H.D. Kim, T.H. Kim, W. Jo, Differences in nature of defects between $SrBi_2Ta_2O_9$ and $Bi_4Ti_3O_{12}$, Applied Physics Letters 74 (1999) 1907–1909.
[60] I. Coondoo, A.K. Jha, S.K. Aggarwal, Enhancement of dielectric characteristics in donor doped Aurivillius $SrBi_2Ta_2O_9$ ferroelectric ceramics, Journal of European Ceramic Society 27 (2007) 253.
[61] A. Chen, Y. Zhi, L.E. Cross, Oxygen-vacancy-related low-frequency dielectric relaxation and electrical conduction in $Bi:SrTiO_3$, Physical Review B 62 (2000) 228–236.
[62] Y. Noguchi, M. Miyayama, K. Oikawa, T. Kamiyama, M. Osada, M. Kakihana, Defect engineering for control of polarization properties in $SrBi_2Ta_2O_9$, Japanese Journal of Applied Physics 41 (Part 1) (2002) 7062.
[63] W.L. Warren, D. Dimos, B.A. Tuttle, Electronic and ionic trapping at domain walls in $BaTiO_3$, Journal of the American Ceramic Society 77 (1994) 2753.
[64] Q.Y. Jiang, L.E. Cross, Effects of porosity on electric fatigue behaviour in PLZT and PZT ferroelectric ceramics, Journal of Materials Science 28 (1993) 4536.
[65] J.F. Scott, C.A. Araujo, B.M. Melnik, L.D. McMillan, R. Zuleeg, Quantitative measurement of space charge effects in lead zirconate titanate memories, Journal of Applied Physics 70 (1991) 382.
[66] Sugandha, A.K. Jha, Investigations of dielectric and ferroelectric properties of yttrium substituted $SrBi_2Ta_2O_9$ ferroelectric ceramics, in: Proceedings of IEEE, 2012, ISBN:978-1-4673-2668-1.
[67] Sugandha, A.K. Jha, Effect of sintering temperature on the microstructural and electrical properties of non stoichiometric strontium bismuth tantalate ferroelectric ceramics, Indian Journal of Physics 87 (4) (2013) 325–331.
[68] M. Yamaguchi, T. Nagamoto, O. Omoto, Preparation of highly c-axis-oriented $Bi_4Ti_3O_{12}$ thin films and their crystallographic, dielectric and optical properties, Thin Solid Films 300 (1997) 299.